Competition Between Neutron and Gamma-Ray Emission Following Formation of the Compound Nucleus Po^{210} in the Systems Pb^{206}+α and Bi^{209}+p†

J. Robb Grover

Chemistry Department, Brookhaven National Laboratory, Upton, New York

AND

Richard J. Nagle

Lawrence Radiation Laboratory, University of California, Livermore, California

(Received 4 February 1964)

We report measurements of the cross-section ratio $R_x = \sigma(\text{Po}^{208})/[\sigma(\text{Po}^{208}) + \sigma(\text{Po}^{209})]$ for the reactions Pb$^{206}(\alpha,n)$Po^{209}, Pb$^{206}(\alpha,2n)$Po^{208}, and Bi$^{209}(p,n)$Po^{209}, Bi$^{209}(p,2n)$Po^{208} for bombarding energies up to 2.7 and 2.3 MeV above the respective $\alpha,2n$ and $p,2n$ thresholds. The shape of R_α as a function of energy is clearly different from the shape of R_p. Moreover, using threshold energies determined "internally" by extrapolation of the data we show that $R_\alpha > R_p$ at any given excitation energy of the Po^{210} compound nucleus over the entire range of energies studied. Despite this observed dependence of decay on the mode of formation, we find that our results are completely consistent with the compound nucleus mechanism if we take into account (1) the competition between gamma-ray emission and neutron emission, and (2) the different distributions of angular momenta characterizing the compound nucleus Po^{210} for the two different target-projectile systems. From a detailed analysis of the data nearest threshold we find the value of the level density parameter a to be about 11 MeV^{-1} (to within about ±20%), in agreement with values of a from other types of data in the mass region $A = 204$ to 210. Simultaneously we also obtain an estimate for the ratio of mean radiation width to mean level spacing in Po^{209} at excitation energies near the neutron binding energy, which estimate agrees well with the value expected from systematics. We also report measurements of the ratio $\mathcal{R}_\gamma = \sigma(\text{Po}^{210})/[\sigma(\text{Po}^{208}) + \sigma(\text{Po}^{209}) + \sigma(\text{Po}^{210})]$ where the Po^{210} is formed in the Bi$^{209}(p,\gamma)$Po^{210} reaction.

INTRODUCTION

EVIDENCE for the emission of gamma rays in competition with particle emission should often be seen prominently in excitation functions for products formed by particle emission from a compound nucleus.[1,2] The importance of this competitive gamma-ray emission is qualitatively revealed by the following aspects of the experimental data: (1) by systematic differences in behavior among excitation functions for reactions induced by heavy ions, helium ions, and smaller particles,[2-5] (2) by apparent inconsistencies between excitation functions or activation measurements and particle spectra,[6,7] and between excitation functions and the angular distributions of the recoiling product nuclei,[8,9] and (3) by the apparently too copious gamma-ray production in bombardments with heavy ion projectiles.[10] More quantitatively, the importance of such competition is demonstrated by the analyses of excitation functions that have been carefully measured within one or two MeV above threshold, where the product levels are known so that the required calculations can be carried out in detail.[1]

However, from the threshold analyses it is found that the data are consistent not only with "sensible" values of the state density parameter a and of the radiation-width parameter $b(0)$ (both defined below), but also with a very wide range of other value-pairs of a and $b(0)$ as well. Since recognition of the importance of competitive gamma-ray emission is often a decisive factor in one's ideas of how data on nuclear reactions ought to be measured and interpreted, stronger experimental verification is desirable. An experiment is described in this report, the results of which we believe help to provide such verification.

One consequence of the competitive gamma-ray emission which suggests an experimental test is that independence of formation and decay of the compound nucleus should often be *apparently* violated for excitation functions. Let $\sigma_a(X)$ and $\sigma_a(Y)$ be the cross sections for the formation of products X and Y by the emission of particles and photons from the compound nucleus C formed by amalgamation of the target nucleus A and projectile a, and let $\sigma_b(X)$ and $\sigma_b(Y)$ be the corresponding cross sections for target nucleus B and projectile b. Independence of formation and decay of the compound nucleus would require, as a first approximation, that[11]

$$\sigma_a(X)/\sigma_a(Y) = \sigma_b(X)/\sigma_b(Y), \qquad (1)$$

† Research performed under the auspices of the U. S. Atomic Energy Commission.

[1] J. R. Grover, Phys. Rev. **123**, 267 (1961).

[2] J. R. Grover, Phys. Rev. **127**, 2142 (1962).

[3] A. S. Karamyan, Yu. B. Gerlit, and B. F. Myasoedov, Zh. Eksperim. i Teor. Phys. **36**, 621 (1959) [English transl.: Soviet Phys.—JETP **9**, 431 (1959)].

[4] J. M. Alexander and G. N. Simonoff, Phys. Rev. **133**, B93 (1964); *ibid.* **130**, 2383 (1963).

[5] G. R. Choppin and T. J. Klingen, Phys. Rev. **130**, 1990 (1963).

[6] G. Igo and H. E. Wegner, Phys. Rev. **102**, 1364 (1956).

[7] R. N. Glover and E. Weigold, Nucl. Phys. **29**, 309 (1962).

[8] G. N. Simonoff and J. M. Alexander, Phys. Rev. **133**, B104 (1964).

[9] J. R. Morton, III, G. R. Choppin, and B. G. Harvey, Phys. Rev. **128**, 265 (1962).

[10] J. F. Mollenauer, Phys. Rev. **127**, 867 (1962).

[11] S. N. Ghoshal, Phys. Rev. **80**, 939 (1950).

provided the compound nuclei from the two systems are at the same excitation energy. However, we must remember that the "compound nucleus" made in these reactions is distributed over a spectrum of angular momenta $j\hbar$, and that in general the distribution of angular momenta for the reaction of A with a, $P_a(j)$, will be different from the corresponding distribution for the reaction of B with b, $P_b(j)$. Thus, letting $F(j,X)$ and $F(j,Y)$ represent the fraction of the compound nuclei with angular momentum $j\hbar$ which eventually form X and Y, respectively, it is clear that Eq. (1) is more correctly written as an inequality,[12]

$$\frac{\sigma_a(X)}{\sigma_a(Y)} = \frac{\sum_j P_a(j)F(j,X)}{\sum_j P_a(j)F(j,Y)}$$

$$\neq \frac{\sum_j P_b(j)F(j,X)}{\sum_j P_b(j)F(j,Y)} = \frac{\sigma_b(X)}{\sigma_b(Y)}. \quad (2)$$

Although Ghoshal's experiment[11] demonstrates the practical validity of Eq. (1) for the particular systems and for the relatively poor (by present-day standards) accuracy with which he worked, Eq. (2) predicts that Eq. (1) would in general be violated for experiments performed accurately enough to be sensitive to differences between[13] $P_a(j)$ and $P_b(j)$ in those cases where $F(j,X)$ and/or $F(j,Y)$ vary strongly with j. Competitive gamma-ray emission often strongly influences this inequality, especially when more than one particle is emitted from C to form X and/or Y, and for such reactions we can usually predict quite easily which side should be the larger for a given pair of systems (an example of such a prediction is given further on).

The two parameters mentioned in the first paragraph, in terms of which the results of an excitation function measurement may be expressed, are (i) the state density parameter a, where the state density (summed over angular momenta) is given, e.g., by[14]

$$\rho(E) \approx \text{const.} (E+t)^{-5/4} \exp[2(aE)^{1/2}], \quad (3)$$

E being the nuclear excitation energy, with the thermodynamic temperature t given approximately by $E = at^2 - t$, and (ii) a parameter $b(0)$, which is the ratio of average radiation width $\bar{\Gamma}_\gamma(J^\pi,E)$ to average level spacing $D(J^\pi,E)$ evaluated at some convenient excitation energy (usually the neutron binding energy B_n) and at a spin-parity J^π equal to zero-even (fictional, of course, for an odd-mass nucleus), i.e., $b(0) = \bar{\Gamma}_\gamma(0^+,B_n)/D(0^+, B_n)$. Although there appears to be no unique pair of values $a,b(0)$ in terms of which a given excitation function may be expressed, the locus of acceptable pairs does define a smooth curve when plotted out on a graph having the coordinates a and $b(0)$.[1] Using the analytical procedure described in Ref. 1, it is found that such curves should in general be different for reactions in which the same products are formed as a result of particle evaporation from the same "compound nucleus" prepared with different target-projectile systems. Furthermore, the curves should intersect at a single point, and the point of intersection should give simultaneously the values for a and $b(0)$. The experiment described below was carried out to test these specific predictions, also.

CHOICE OF EXPERIMENT

The reaction systems studied are $\text{Pb}^{206}(\alpha,2n)\text{Po}^{208}$, $\text{Pb}^{206}(\alpha,n)\text{Po}^{209}$, and $\text{Bi}^{209}(p,2n)\text{Po}^{208}$, $\text{Bi}^{209}(p,n)\text{Po}^{209}$. There are several reasons why these reactions are especially suitable for the proposed experiment. (i) Reasonably pure target materials are easily obtainable. (ii) The yields of both Po^{208} and Po^{209} can be measured by pulse analysis of the alpha particles emitted in their decays. (iii) Charged particle emission and fission can be neglected. (iv) The reactions quite probably proceed by an almost pure compound nucleus mechanism.[15] (v) There exists sufficient information about the first few levels of Po^{208} to allow detailed analysis of the data up to about 1 MeV above threshold. (vi) The reactions $\text{Bi}^{209}(p,n)\text{Po}^{209}$ and $\text{Bi}^{209}(p,2n)\text{Po}^{208}$ have previously been studied near the $p,2n$ threshold,[16] and these data form the backbone of the threshold-analysis[1] evidence cited in the first paragraph of this paper; it would therefore be wise to confirm them. (vii) The half-life of Po^{209} (103 yr) is just enough longer

---

[12] We treat $F(j,X)$ and $F(j,Y)$ as if they were independent of the way in which the compound nucleus is formed. This is not exactly true since these properties of the "compound nucleus" are averages over many levels within the experimental energy resolution. For example, the partial widths of these levels with respect to any given channel of de-excitation are nonuniform, having a broad distribution, while in general their relative population will be different for different target-projectile systems. The F's more closely approach independence of the mode of formation the more levels that are included in the averaging, except that there is always at least a slight preference for compound elastic scattering, because those levels having large partial widths for re-emission into the entrance channel are just those which will tend to be preferentially populated in the compound nucleus. In our experiment these effects are expected to be very small, and are neglected. Discussions relevant to these matters may be found in the following papers: P. A. Moldauer, Phys. Rev. 123, 968 (1961); G. R. Satchler, Phys. Letters 7, 55 (1963).

[13] See also the paper by W. John, Phys. Rev. 103, 704 (1956), who points out that for Ghoshal's and for his own data Eq. (1) very likely is not valid. However, the data he used are not quite accurate enough to allow a firm conclusion.

[14] D. W. Lang, Nucl. Phys. 42, 353 (1963); Ref. 38; and the papers cited in footnotes 9 and 19 of Ref. 1, and footnote 18 of Ref. 2.

[15] One expects this, because the energy regions in which these reactions are studied (20 to 23 MeV for $\alpha+\text{Pb}^{206}$ and 10 to 13 MeV for $p+\text{Bi}^{209}$) are near the Coulomb barrier in each case, a condition unfavorable for knockout or other direct reaction mechanisms. The incident particles are strongly "focused" toward the interior of the nucleus [R. M. Eisberg, I. E. McCarthy, and R. A. Spurrier, Nucl. Phys. 10, 571 (1959)] which disfavors the direct knockout of nucleons from the nuclear surface since the knocked-on nucleons would tend to be directed more deeply into the nuclear matter rather than away from the nucleus. Also, the de Broglie wavelength becomes large compared to nuclear dimensions for the slowed-down projectiles near the top of the barrier, and this additionally disfavors any tendency of the projectiles to interact strongly with individual target-surface nucleons.

[16] C. G. Andre, J. R. Huizenga, J. F. Mech, W. J. Ramler, E. G. Rauh, and S. R. Rocklin, Phys. Rev. 101, 645 (1956).

than that of Po^{208} (2.9 yr) that small amounts of Po^{208} can be measured in the presence of large amounts of Po^{209}, while Po^{209} itself is still easily measurable.

For this experiment, we are not really interested in the absolute values of the cross sections, but rather in the ratio of cross sections for Po^{208} and Po^{209}. It proves convenient to define the ratios in the form $R_\alpha(\mathscr{E})$ and $R_p(\mathscr{E})$, where

$$R_x(\mathscr{E}) = \sigma_x(Po^{208})/[\sigma_x(Po^{209}) + \sigma_x(Po^{208})]; \quad (4)$$

the x,n and $x,2n$ cross sections are designated, respectively, by $\sigma_x(Po^{209})$ and $\sigma_x(Po^{208})$, and $\mathscr{E}$ is the center-of-mass bombarding energy in excess of threshold for the $x,2n$ reaction. The ratios R_x are quite sensitive to the competition between gamma-ray emission and particle emission in the de-excitation of the excited Po^{209} resulting from the emission of the first neutron from the "compound nucleus" Po^{210}. Therefore the principal effort of this experiment was to measure $R_x(\mathscr{E})$ as accurately as possible.

To measure R_x we required accurate measurements only of the *relative* production of Po^{208} and Po^{209} (which measurements are particularly easy to make using alpha pulse-height analysis), and of the relative-energy scale in the region from the $x,2n$ threshold to about 2 to 3 MeV higher. The absolute threshold need not be accurately determined to obtain accurate values of $\mathscr{E}$; the quantities which must be accurately determined are the bombarding-energy *differences* between measurements of R_x at successively higher energies. Accurate values of $\mathscr{E}$ can then be found with respect to the relative threshold energy E_{th}, because E_{th} can be determined by a suitable extrapolation of the data.

Activation of a stack of thin foils in a monoenergetic beam of projectiles fulfills the above energy requirements if the energy-straggling can be kept small enough. The energy-difference measurements may then be related to the foil thicknesses, since many exposures are made in a single run. As only relative-cross-section measurements for production of isotopes are important, it is not necessary to determine the chemical yield of the "radiochemical processing," and this frequently troublesome source of error is eliminated.

TECHNICAL DETAILS

Targets

Lead enriched[17] to 99.85% Pb^{206}, dissolved in an aqueous 2.4% sulfamic acid solution, was electroplated onto pretreated (immersed in 10% nitric acid for three minutes, rinsed with water, dried) 0.0001-in. nickel foils,[18] using a platinum anode and a current of 4 mA,

to form a circular deposit of metallic lead 1.9 cm in diameter. The thinnest plate used had an average surface density of lead of 95 $\mu g/cm^2$ and the thickest, 442 $\mu g/cm^2$.

Metallic bismuth was evaporated *in vacuo* onto 0.0001-in.-thick nickel foils to form deposits with surface densities ranging from 193 to 371 $\mu g/cm^2$.

The average thickness of each lead deposit, and of each bismuth deposit, over the region irradiated by the incident beam, was measured to an accuracy of $\pm 5\%$ using an L x-ray fluorescence technique (calibrated by chemical analysis of some of the foils).

The values of a and $b(0)$ obtained from the analysis of our experimental data are extraordinarily sensitive to the thicknesses and uniformities of the target foils. We therefore made measurements to find out how accurately we knew the target thicknesses and to obtain a reliable knowledge of the extent of the nonuniformities. These measurements are described in the following paragraphs.

We knew the average thickness of each nickel backing foil to about $\pm 0.8\%$, or perhaps slightly better, through our measurements of its area and mass. However, these foils had areas of 10–15 cm^2, while the incident beam irradiated a circular spot only about 1 cm in diameter. To determine the accuracy with which our average-thickness values represented the foil thicknesses actually presented to the beam, we used a $\frac{3}{8}$-in. punch of known area to sample many of the foils (it was too late to make these measurements on the actual irradiated spots, as these portions of the target foils had already been destroyed in the post-bombardment chemical processing) and weighed the punchings with a micro-balance. For the lead foils, we found that we effectively knew the backing-foil thicknesses only to $\pm 2.3\%$; the corresponding accuracy for the bismuth foils was much better, being about $\pm 0.9\%$. Direct measurements of the three aluminum foils (see following subsection) next above threshold in the $Bi^{209} + p$ bombardments were performed to an accuracy of $\pm 0.6\%$, and for the rest of the Al foils used we claim $\pm 1.4\%$. For the foil next above threshold in each of the two $Pb^{206} + \alpha$ bombardments it is desirable to have better accuracy if at all possible; we were able to obtain three punchings from one of these foils and four from the other, but are nevertheless able to claim only insignificantly improved accuracy, $\pm 2.1\%$. We show in a following section that this is the most important limitation of accuracy in the lead bombardments.

We needed to know the nonuniformity of the foil thickness on a scale small compared to 1 cm, in order to calculate the energy-profile of the incident beam as seen by each foil, and we also needed to know the accuracy with which the nonuniformity is known. To obtain these facts we measured the energy-spreading of a beam of the 5.30-MeV alpha particles emitted by a thin deposit of Po^{210} (4 mm in diameter) after it had

---

[17] The isotopically enriched lead 206 was obtained from Oak Ridge National Laboratory, who also provided the following isotopic analysis of the material (expressed as atom percent): 204, <0.02; 206, 99.85; 207, 0.15; 208, <0.02.

[18] The 0.0001-in. nickel foil was supplied by the Chromium Corporation of America, Waterbury, Connecticut.

passed through a target foil (we sampled eight lead foils, two bismuth foils). The Po[210] source was located 4.4 cm from the foil, on a line perpendicular to the plane of the foil and passing through the center of the circular area being tested, which was 1 cm in diameter. The energy profile of the alpha particles after passing through the foil was measured using a solid-state detector and pulse-height analyzer. The linewidth with no foil in place was about 35 keV full width at half-maximum (fwhm). The energy spread observed for 1.27 mg/cm^2 of air between the source and detector was measured to be 60.1±1.2 keV fwhm (the cited uncertainty refers only to reproducibility) and calculated by the theory of Bethe and Ashkin[19] to be 55.3 keV fwhm (corrections for the "geometry" of the system are included). This is sufficiently good agreement[20] that we assume it is accurate enough for our purpose to ascribe to the foil thickness nonuniformity that part of the energy spread not accounted for by Bethe and Ashkin's theoretical prediction. The foil thickness nonuniformity was calculated from the energy spread due to the nonuniformity using the range-energy tables of Williamson and Boujot.[21]

For the lead deposits, the nonuniformity, expressed as fwhm, depended roughly linearly on the average deposit thickness, being about 2.4±0.7 mg/cm^2 per mg/cm^2 of average deposit thickness. This surprisingly high value suggests that the lead deposits were very rough (far rougher than they looked to the eye), and this was seen to be so when the deposits were examined through a microscope. The assigned uncertainty of ±0.7 is the rms deviation of values for individual foils; it is necessary to know this since the above measurements could not be made on the targets actually bombarded but were made instead on a sample of eight targets not irradiated (these eight were selected at random from the original batch of 24 targets, at a time when we did not expect to be making these extra measurements, so there is no reason to suspect that they do not constitute a valid sample). It is, of course, also necessary to know the standard error of the above mean value of 2.4, and that is ±0.2$_4$. The corresponding value for the bismuth deposits is 0.8±0.2 mg/cm^2 fwhm per mg/cm^2 of average deposit thickness, the standard error of the mean being ±0.2. For the nickel backings of the lead targets we found an inverse relationship between

the nonuniformity and the mean foil thickness, as if the surface roughness had increased in proportion to the amount of chemical attack in the plating procedure. The measured nonuniformities were fitted with the empirical formula

$$\mathcal{Y} = 0.704 - 0.221 \mathcal{X} \qquad (5)$$

where $\mathcal{Y}$ is the nonuniformity in mg/cm^2 fwhm, and $\mathcal{X}$ is the average Ni foil thickness in mg/cm^2; the range of thicknesses used was 1.6 to 2.2 mg/cm^2. The rms deviation from $\mathcal{Y}$ of individual values is ±0.031 mg/cm^2, and the standard error of $\mathcal{Y}$ itself is ±0.010 mg/cm^2. For the nickel backings (three samples) of the bismuth targets the measured nonuniformity was nearly constant at 0.141±0.009 mg/cm^2 fwhm. The striking difference between the nickel backing foils for the lead targets and those for the bismuth targets, both in the nonuniformity measurements and in the uncertainty of our knowledge of the foil thicknesses actually seen by the beam, almost surely reflects the effects of chemical attack on the nickel foils in the lead electroplating procedure. Finally, for the 0.0005-in. aluminum foils used between the bismuth targets as energy-degrading foils, the measured nonuniformity was 0.324±0.003 mg/cm^2 fwhm.

Examples of contributions to the energy-profile of the incident beam from foil nonuniformities are presented in the next subsection.

Irradiations

Irradiations were performed *in vacuo* on stacks of eight target foils at a time. The target foils were kept separated from one another by copper spacers $\frac{1}{32}$-in. thick, these spacers also helping to cool the foils. In the proton bombardment of bismuth, a 0.0005-in. aluminum foil was inserted on the downstream side of each target foil, to adjust the total energy degradation of the beam in the entire stack to about 1 MeV. The target foils were so arranged that the thinner Pb[206] and Bi[209] deposits were upstream (i.e., at higher energies) with respect to the thicker deposits.

The irradiations were performed with collimated (to a diameter of $\frac{1}{4}$ in.), magnetically analyzed particle beams from the Livermore 90-in., variable-energy cyclotron. We used the energy-analyzing and collimation systems developed by J. Benveniste *et al.*, which they have described elsewhere.[22] Our target-foil stack was mounted inside their Faraday-cup housing.

The beam energy was measured using their variable absorber "ranger" (foil wheel) plus double proportional counter and anticoincidence circuit to measure the range of particles scattered out of the incident beam at an angle of 30° by a thin (≈ 1 mg/cm^2) nickel foil. The

[19] H. A. Bethe and J. Ashkin, in *Experimental Nuclear Physics*, edited by E. Segrè (John Wiley & Sons, New York, 1953), Vol. I, p. 166.

[20] This datum is not a test of Bethe and Ashkin's theory, for we did not align our apparatus carefully enough for that; however, the small errors of positioning in the air measurement do not affect the foil measurements. Energy-straggling theory seems seldom to have been carefully tested by experiment; the data of W. E. Bennett, Proc. Roy. Soc. (London) **A155**, 419 (1936), for the energy-straggling of 8-MeV alphas passing through mica, agree with Bethe and Ashkin's theory to within the cited experimental error of ±5%.

[21] C. Williamson and J. P. Boujot, Centre D'Études Nucléaires de Saclay, Rapport CEA-2189, 1962 (unpublished).

[22] J. Benveniste, A. C. Mitchell, and C. B. Fulmer, Phys. Rev. **129**, 2173 (1963); J. Benveniste, R. Booth, and A. Mitchell, University of California Radiation Laboratory Report UCRL 7427, July, 1963 (unpublished).

observed ranges were converted to energies using the range-energy tables of Williamson and Boujot[21]; the latter tables were also used to calculate the incident energy seen by each target foil in the target stack.

The energy was held constant during each run using Benveniste et al.'s "continuous energy monitor."[22] This instrument is sensitive enough to record changes in beam energy of less than 0.05%, but in practice, long-term drifts in the associated electronic circuitry limited the energy control to ±0.2%.

The energy profile of the beam before encountering the stack of target foils was measured on particles scattered out of the beam at an angle of 50° by a thin (≈ 1.5 mg/cm^2) gold foil, the energy spectrum being recorded with a p-n junction diode and pulse-height analyzer. The apparent full width at half-maximum due only to noise in the counter-amplifier system was measured to be 65 keV, in terms of beam energy.

To illustrate the relative importance of the various contributions to $W_{1/2}$, the full width at half-maximum of the incident beam seen by the targets, we describe two examples. (1) In the first Pb^{206}+α run (see Table I) for the point at 20.29 MeV, $W_{1/2}=311\pm12$ keV. This is composed of the following contributions (all energies are in center-of-mass coordinates): (a) beam profile before entering the foil stack (including long-term drift), 171 ± 11 keV fwhm; (b) lead deposit nonuniformity, 167 ± 18 keV fwhm; (c) nickel backing nonuniformity, 112 ± 7 keV fwhm; (d) theoretical energy straggling,[19] 165 keV fwhm. (2) For Bi^{209}+p at 9.84 MeV, $W_{1/2}=148\pm4$ keV fwhm, composed of the following contributions: (a) beam profile before entering the foil stack, 66 ± 7 keV fwhm; (b) foil nonuniformity, 29 keV fwhm; (c) theoretical, 130 keV fwhm. We do not know how accurate the values calculated by the energy straggling theory of Bethe and Ashkin[19] are, partly because we don't know what values of k_n (their notation) to use in the calculations (we used $k_n=1$ at these high energies and $k_n=\frac{4}{3}$ for the 5-MeV alphas), and partly because of the paucity of experimental verifications of the theory. Our best judgment is that the theoretical values we use are very likely more accurate than ±10% but probably not better than ±5%. If we assume ±7.5% and fold this additional contribution into the above Pb^{206}+α point, we obtain 311 ± 14 keV fwhm, which is not a serious increase in uncertainty compared to the other experimental uncertainties (e.g., see Table II). The uncertainty in the theory is even less serious for the Bi^{209}+p system (see Table II).

The protons were accelerated in the cyclotron as H$^+$ ions, and not as H$_2^+$ ions, so contamination of the beam with deuterons was not troublesome.

The intensity of the irradiations was held to $\leqslant 0.15$ μA, in order to avoid melting the lead or bismuth, which would risk volatilizing the product polonium. In the alpha bombardments we pulse-analyzed the downstream surfaces of two target foils, to test for volatiliza-tion and redeposition of Po, and negligible Po alpha-radioactivity was detected (roughtly 10^{-3} the counting rate of the facing target). Total irradiations of about 1000–2000 microcoulombs were performed in each of the bombardments; no attempt was made to measure the integrated beam current accurately.

Chemistry

The product polonium was chemically separated from the targets and plated on flamed platinum disks as "weightless" deposits,[23] to facilitate the alpha pulse-analysis. In a 40-ml glass centrifuge cone, the target with its nickel backing foil was dissolved in 4 ml of boiling concentrated hydrochloric acid containing four drops of 4N nitric acid, and the solution twice boiled to saturated solution, first with addition of 1 ml of concentrated hydrochloric acid, and again after washing down the sides of the cone with 0.1N hydrochloric acid. Finally the solution was made up to six ml in dilute hydrochloric acid (0.1N HCl for lead and about 0.35 to 0.4N HCl for bismuth—i.e., the lowest concentration of HCl at which the cloudiness of the solution just clears up), poured into a Lucite plating cell the bottom of which was the flamed platinum disk, and hydrogen gas was bubbled through the solution for about one hour. Finally, the platinum disk, on the surface of which most of the polonium had been deposited, was washed with distilled water, then with absolute ethanol, and dried in air.

Counting

The alpha pulse-analysis of the Po plates was performed in a Frisch grid ionization chamber, the energy spectrum being recorded with a pulse-height analyzer. The resolution of the ion chamber-amplifier-pulse height analyzer set up was 35 keV full width at half-maximum, and the background was around 6 counts per day per channel 10 keV wide. The counting rates were such that the background correction seldom exceeded 5%, and was about 11% at worst. The reproducibility of the counting was consistent with the number of counts collected in the peaks (seldom less than 3000 and never less than 500; in addition, we counted every plate at least twice). Independent analyses of the data by the two authors almost always was in agreement to within a few tenths of a percent, so it is thought that the most serious counting uncertainty is statistical.

EXPERIMENTAL DATA

The experimental data are presented in Table I. The first column identifies the particular run. The nominal

[23] R. J. Nagle, unpublished work based on the following reports: O. Erbacher, Z. Physik. Chem. 156A, 142 (1931); R. J. Prestwood, U. S. Atomic Energy Commission Report AECD-2839, 1944 (unpublished).

TABLE I. Experimental data. $R_x = \sigma_x(Po^{208})/[\sigma_x(Po^{208})+\sigma_x(Po^{209})]$ and $\mathcal{R}_\gamma = \sigma_x(Po^{210})/[\sigma_x(Po^{208})+\sigma_x(Po^{209})+\sigma_x(Po^{210})]$.

Run	Bombarding energy (MeV, c.m.) E_b	$W_{1/2}$ (keV) fwhm	$10^3 R_x$	ΔE (keV)	$10^3 R_x$ corrected	$10^3 \mathcal{R}_\gamma$ [a]
Pb+α	19.964		<0.06			5.29
	20.290	311±12	4.37 ±0.14	54	4.19 ±0.14	5.11
	20.672	279±12	30.25 ±0.29	18	29.87 ±0.29	4.76
	21.034	254	78.5 ±0.8	9	78.1 ±0.8	4.41
1st bombardment	21.416	232	144.1 ±1.3	5		3.44
	21.807	212	225.2 ±1.3			2.48
	22.145	191	319.7 ±2.6			2.31
	22.486	171±11	421.7 ±4.5			1.98
Pb+α	20.237	321±12	3.68 ±0.06	61	3.51 ±0.06	3.93
	20.632	296±12	28.49 ±0.30	20	28.08 ±0.30	3.59
	20.985	272	72.2 ±0.6	10	71.8 ±0.6	3.14
	21.343	252	135.3 ±1.1	6		2.60
2nd bombardment	21.712	233	210.8 ±2.4			2.24
	22.053	214	298.4 ±2.6			2.01
	22.448	193	401.4 ±1.8			2.28
	22.767	171±9	506.0 ±2.6			1.54
Bi+p	9.665	158	<0.05			1.325±0.015
	9.843	148±4	0.599±0.025	20	0.587±0.025	1.349±0.010
	10.020	138±4	3.331±0.055	10	3.309±0.055	1.301±0.015
	10.194	127±4	8.85 ±0.11	5	8.81 ±0.11	1.275±0.016
3rd bombardment	10.371	115±5	17.66 ±0.23	3		1.317±0.015
	10.540	101	29.76 ±0.24			1.319±0.017
	10.709	86	48.22 ±0.38			1.321±0.018
	10.879	66	72.8 ±0.7			1.295±0.022
Bi+p	10.809		62.7 ±0.5			1.335±0.019
	10.975		87.7 ±0.5			1.290±0.013
	11.138	similar	118.1 ±0.9			1.241±0.017
	11.299	to	155.1 ±1.1			1.241±0.016
4th bombardment	11.460	3rd	201.3 ±0.9			1.198±0.014
	11.618	bombard-	252.8 ±1.2			1.188±0.016
	11.775	ment	308.2 ±2.4			1.143±0.015
	11.931		360.9 ±2.3			1.101±0.009

[a] The statistical errors on $\mathcal{R}_\gamma$ for the Pb^{206}+α bombardments are about ±1.5% except for ±2.5% for the highest energy point of the 1st bombardment.

bombarding energy E_b at each target in column two is given to the nearest 0.001 MeV, because it is the differences between successive energies which must be known accurately in this experiment; the absolute adjustment of the whole energy scale is not known more closely than about ±1%, partly because the range-energy relations are not known with an accuracy much better than 1%, and partly because we did not calibrate the "ranger" absolutely and so do not know its end-correction. The relative-energy adjustment between the two Bi^{209}+p runs is known to within ±0.015 MeV, however. The third column gives the full width at half-maximum of the energy profile of the incident beam $W_{1/2}$ at each target foil, calculated from the various contributions measured as described in the section entitled "Technical Details." The fourth column gives the measured apparent values of $R_x = \sigma_x(Po^{208})/[\sigma_x(Po^{208})+\sigma_x(Po^{209})]$; the assigned uncertainties reflect only the counting statistics and neglect uncertainties in the half-lives and decay schemes of Po^{208} and Po^{209}. The fifth column gives the energies ΔE which should be added to the values in column two, relevant to the excitation function for the production of Po^{208}, to correct for the

spread in energy of the incident beam. The method we used to make this beam-profile correction is described in the Appendix. The corresponding correction for Po^{209} is very small and was neglected. Finally, in column six are given the values of R_x relevant to the energy values of column two corrected according to column five; here we take account of the change in the cross section for the formation of Po^{209} in proceeding to the corrected incident energy. In column seven we present our measured values for $\mathcal{R}_\gamma = \sigma(Po^{210})/[\sigma(Po^{210})+\sigma(Po^{209}) +\sigma(Po^{208})]$ relevant to the energy values in column two.

We used the following data in converting our measurements to the form given in Table I. The half-lives of Po^{208}, Po^{209}, and Po^{210} were taken to be 2.897 years, 103 years, and 138.4 days,[24] and their alpha decay abundances to be 100%, 99.1%, and 100% for the alpha lines of energies 5.11, 4.88, and 5.30 MeV, respectively.[25]

[24] P. E. Figgins, U. S. Atomic Energy Commission Report NAS-NS-3037 (unpublished).
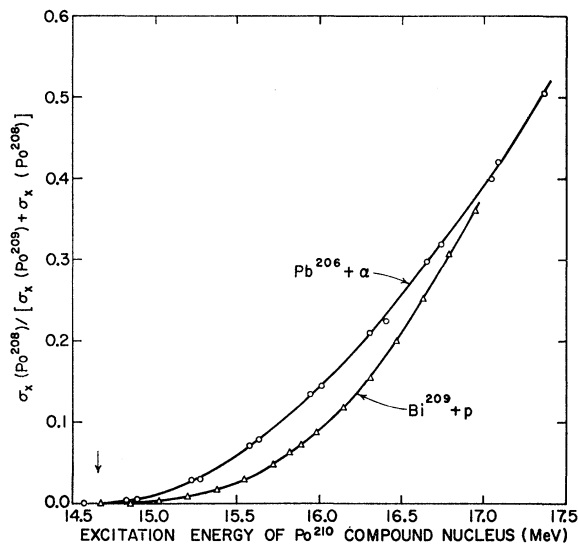[25] D. Strominger, J. M. Hollander, and G. T. Seaborg, Rev. Mod. Phys. 30, 585 (1958).

FIG. 1. Experimentally measured values of $R_x = \sigma_x(\mathrm{Po}^{208})/$ $[\sigma_x(\mathrm{Po}^{208}) + \sigma_x(\mathrm{Po}^{209})]$ plotted as a function of the excitation energy of the Po^{210} compound nucleus, for both target-projectile systems. The $x,2n$ threshold corresponds to an excitation energy of 14.65 MeV (arrow at lower left). The lines are merely drawn through the points and have no theoretical significance. The circles are for the alpha bombardments of Pb^{206} and the triangles are for the proton bombardments of Bi^{209}.

The 0.15% of Pb^{207} in the separated Pb^{206} we used would contribute to the yield of Po^{209} by the $\mathrm{Pb}^{207}(\alpha,2n)\mathrm{Po}^{209}$ reaction, the threshold for which is 19.83 MeV (c.m.) compared with a threshold of 20.06 MeV for the reaction $\mathrm{Pb}^{206}(\alpha,2n)\mathrm{Po}^{208}$. If we disregard the above figure of 0.15% and estimate the upper limit of the content of Pb^{207} from our observed relative yield of Po^{210}, which can be made in the reaction $\mathrm{Pb}^{207}(\alpha,n)\mathrm{Po}^{210}$ (we describe how we made this estimate, in another section), we obtain upper limits of 0.4% in the first bombardment and 0.3% in the second. Thus, at worst the correction to our measured values of R_α, which correction would be highest at the highest energies studied, should not exceed 0.8%, and has therefore been neglected. Contributions to the formation of Po^{208} via the reaction $\mathrm{Pb}^{204}(\alpha,\gamma)\mathrm{Po}^{208}$ induced in Pb^{204} impurity are entirely negligible.

ANALYSIS OF THE DATA

Qualitative Analysis

In Fig. 1 are plotted the experimentally measured values of R_x given in column four of Table I versus the excitation energy of the Po^{210} compound nucleus. These excitation energy values were calculated from the measured bombarding energies given in column two of Table I, using the relative nuclidic masses published by König et al.[26] This figure demonstrates that

[26] L. A. König, J. H. E. Mattauch, and A. H. Wapstra, Nucl. Phys. 31, 18 (1962).

$\sigma_\alpha(\mathrm{Po}^{208})/\sigma_\alpha(\mathrm{Po}^{209}) \neq \sigma_p(\mathrm{Po}^{208})/\sigma_p(\mathrm{Po}^{209})$, that is, that $R_\alpha(\mathscr{E}) \neq R_p(\mathscr{E})$, consistent with Eq. (2), and in disagreement with Eq. (1). This inequality cannot be explained by the cited $\pm 1\%$ uncertainty in the energy scales because no adjustment of the energy scale for the alpha bombardments with respect to the energy scale for the proton bombardments can bring the two sets of data into alignment; the two curves have quite different shapes. The beam-profile correction changes these curve shapes only a little, and in such a way as to make them even more different.

In Fig. 1 it appears that $R_\alpha(\mathscr{E}) > R_p(\mathscr{E})$. That this impression is true is easily verified. Even crude extrapolations of the data will yield approximate threshold energies which serve to fix the relative-energy-scale adjustment between the $\mathrm{Pb}^{206} + \alpha$ data and the $\mathrm{Bi}^{209} + p$ data considerably more accurately than the range measurements could. Using such extrapolated thresholds we find that indeed $R_\alpha(\mathscr{E}) > R_p(\mathscr{E})$ for the entire range of $\mathscr{E}$ covered in this work.

We can see why $\sigma_\alpha(\mathrm{Po}^{208})/\sigma_\alpha(\mathrm{Po}^{209}) > \sigma_p(\mathrm{Po}^{208})/$ $\sigma_p(\mathrm{Po}^{209})$ for small $\mathscr{E}$ if we take into account the competitive gamma-ray emission. In Fig. 2 are plotted examples of the distributions of angular momenta, $P_\alpha(j)$ and $P_p(j)$, in the compound nuclei Po^{210} resulting from the alpha-particle and proton bombardments, calculated (see next section) to correspond to the same excitation energy of Po^{210}, 14.95 MeV, and normalized so that $\sum_j P_\alpha(j) = \sum_j P_p(j) = 1$. (The strong maximum of $P_p(j)$ at $j(\mathrm{Po}^{210}) = 4$ to 5 appears because the spin of the Bi target is $\frac{9}{2}$, while little angular momentum is carried in by the incident protons.) We do not also
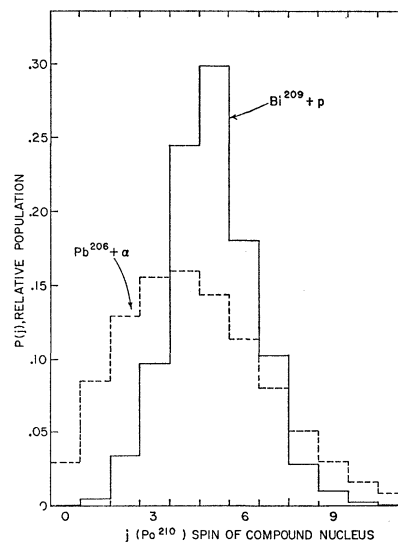

FIG. 2. Normalized relative distributions of Po^{210} compound nuclei with respect to angular momentum $j\hbar$, for the target-projectile systems, $\mathrm{Bi}^{209} + p$ (solid line) and $\mathrm{Pb}^{206} + \alpha$ (dashed line). The bombarding energies for this example are such as to give a Po^{210} excitation energy of 14.95 MeV, i.e., 0.30 MeV above the $x,2n$ threshold.
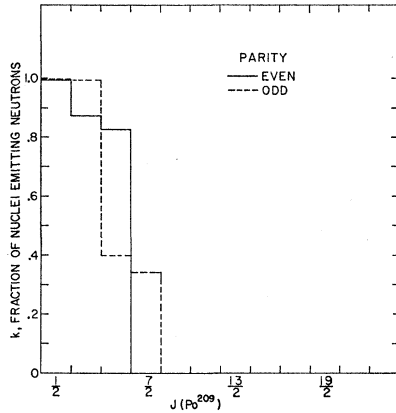
FIG. 3. Fraction of excited Po^{209} nuclei which de-excite by neutron emission to form Po^{208}, when the excitation energy of the Po^{209} is 7.23 MeV (i.e., when the neutrons can only be emitted with 0.27 MeV), plotted as a function of the angular momentum $J\hbar$. The Po^{209} nuclei which do not emit neutrons de-excite by gamma-ray cascades to form ground state Po^{209}. Solid lines denote excited Po^{209} nuclei of even parity and dashed lines denote odd parity. This example was calculated using $a=10.6$ MeV^{-1}, $b(0) = 7.5 \times 10^{-5}$, $\mathcal{I} = \mathcal{I}_r$.

display values of $F(j, \text{Po}^{208})$ and $F(j, \text{Po}^{209})$, because our computer program is not so arranged as to calculate these factors explicitly. However, we can see qualitatively what the F's are like from Fig. 3 which shows the calculated situation (using reasonable input data) for Po^{209} sufficiently excited to emit a 0.27-MeV neutron to populate the ground state (spin-parity=0$^+$) of Po^{208} (Since the first excited state of Po^{208} is at 0.66 MeV, we need not consider excited states.) The abscissa represents the angular momentum of the excited Po^{209} in units of $\hbar$, and the ordinate represents the fraction k of the nuclei that de-excite by the emission of a neutron to become Po^{208}, instead of emitting gamma rays to eventually form the ground state of Po^{209}. We see readily from Fig. 3 that $F(j, \text{Po}^{208})$ is relatively large for $j \lesssim 3$ and falls rapidly for larger j's [while $F(j, \text{Po}^{209})$ varies with j in the complementary sense]. This behavior comes about because for compound nuclei of high spin to reach a product state with zero spin by neutron emission, the neutrons must carry off considerable angular momentum. Beyond some critical magnitude of angular momentum change (about 3 units in this example) the neutron emission rate is sufficiently diminished by the centrifugal barrier to permit gamma-ray emission to predominate. Referring back to Fig. 2, we can see now why R_α should rise from threshold more rapidly than R_p within the first MeV above threshold. It is interesting to observe that if the ground-state spin of Bi^{209} had been $\frac{1}{2}$ instead of $\frac{9}{2}$, $P_p(j)$ would have had its maximum near $j=1$ to 2 instead of near $j=4$ to 5, and our conclusion would have been just the opposite; R_p should then have been predicted to rise faster than R_α.

The nonvalidity of the Ghoshal condition, i.e. Eq. (1), for compound nucleus reactions is thus ap-

parently established by this example, in a way which does not depend on accurate relative energy adjustments between different target-projectile systems. Moreover, we can offer a qualitative explanation within the compound nucleus model which accounts for our observation that $R_\alpha > R_p$ near threshold, in the reactions we studied. We now need to know whether this qualitative explanation holds up under a more quantitative and detailed analysis. The following subsection is the report of such an analysis.

Quantitative Analysis

We analyzed the data according to the prescription given in the section "Calculational Procedure" of Ref. 1. The calculations were performed with the aid of the Brookhaven IBM 7094 computer facility. We first describe the input data chosen for the analysis, then we describe various features of the work and give the results and our conclusions.

Input Data

In this work, we used for the dependence of the level density[14] on angular momentum $J\hbar$,

$$\omega(J,E) = \omega(0,E)(2J+1) \exp[-J(J+1)/2\sigma^2], \quad (6)$$

where

$$\sigma^2 = (\mathcal{I}/\hbar^2)t, \quad (7)$$

where $\mathcal{I}$ is a nuclear moment of inertia, assumed to be that of a rigid sphere $\mathcal{I}_r$, with a radius $R = 1.2 \times 10^{-13} A^{1/3}$ cm. From Eq. (3),

$$\omega(J,E) = (\text{const.})(2J+1)(E+t)^{-2}$$
$$\times \exp[-J(J+1)/(2\sigma^2) + 2(aE)^{1/2}]. \quad (8)$$

In using Eq. (18) of Ref. 1 we retained the J dependence of $f(E_F)$, instead of using the simplification represented by Eq. (16) of that paper.

The transmission coefficients for neutron emission, and for protons incident on Bi^{209} were calculated for the diffuse-surface, surface-absorption potential of Bjorklund and Fernbach,[27] using E. Auerbach's ABACUS-2 code.[28] The parameters used (in the same notation as that in Bjorklund and Fernbach's paper) were the following: for neutrons,[27] $V_{CR} = 50.0$ MeV, $V_{CI} = 7.0$ MeV, $V_{SR} = 9.5$ MeV, $a = 0.65 \times 10^{-13}$ cm, $b = 0.98 \times 10^{-13}$ cm, $r_0 = 1.25 \times 10^{-13}$ cm; for protons,[29] $V_{CR} = 57.6$, $V_{CI} = 11.0$, $V_{SR} = 5.0$, $a = 0.65$, $b = 1.2$, $r_0 = 1.25$. Although in our calculation we neglect the dependence of T_l on the total angular momentum of the system, the ABACUS-2 code provides us with proton and neutron transmission coefficients which depend on

[27] F. Bjorklund and S. Fernbach, Phys. Rev. 109, 1295 (1958).
[28] Dr. E. H. Auerbach graciously supplied us with a copy of the binary deck of ABACUS-2, together with a set of instructions for its use, Brookhaven National Laboratory Report 6562, November, 1962 (unpublished).
[29] F. Bjorklund, G. Campbell, and S. Fernbach, Helv. Phys. Acta, Suppl. VI, 432 (1961).

spin-orbit coupling, $T_{l,l-1/2}$ and $T_{l,l+1/2}$. We obtained averaged transmission coefficients for our calculation from the relation $(2l+1)T_l = lT_{l,l-1/2} + (l+1)T_{l,l+1/2}$. For helium ions incident on Pb^{206}, the transmission coefficients tabulated by Huizenga and Igo[30] were used.

The reaction Q values, -9.64 MeV for $Bi^{209}(p,2n)Po^{208}$ and -20.06 MeV for $Pb^{206}(\alpha,2n)Po^{208}$ were obtained from the tables published by König et al.,[26] as was the value 6.96 MeV for the binding energy of the last neutron in Po^{209}.

Po^{208} is known to have excited states at 0.66 and at 0.84 MeV, and a state which may be either at 0.91 or at 1.09 MeV.[31] The only state for which the spin and parity are known is the ground state ($J^\pi = 0^+$). Although it is not unreasonable to assume a spin-parity of 2+ for the 0.66 MeV state (which we did), the threshold analysis was performed only for incident energies not exceeding 0.72 MeV above threshold, where the contribution from this excited state is still negligible.

We continue to neglect the averaging correction which should be applied to Eqs. (4) and (18) of Ref. 1 to account for the error we make in setting up the problem as ratios of averages rather than average ratios.[32] The effect of such a correction would be to reduce the final values of $b(0)$ that we extract from the data by a factor 1.3 to 1.5. This factor is not so very much smaller than our experimental error which is, roughly, a factor 2.4. If our experiment were to be repeated with the errors reduced to the point presently foreseeable, this correction would be much too large to neglect in the analysis of the resulting data.

The Intersection of the Two $a,b(0)$ Loci

We found that we can readily calculate excitation functions that fit the experimentally determined values of R_p (and presumably R_α) very closely. Such a fit is demonstrated in Fig. 5. However, as was pointed out in Ref. 1, the mere achievement of good fits is still not necessarily meaningful, because they can be achieved over a wide range of pairs of values of the parameters a and $b(0)$. In this experiment, we have therefore imposed an additional requirement, namely, that the fits to the experimental data be achieved simultaneously

for the two different target-projectile systems. The specific question to which we seek an answer is: Can the data be simultaneously fitted with one and only one pair of parameters a, $b(0)$, and, if so, are the resulting values reasonable? As described below, we find that the answer is "yes."

Fig. 4 shows, for both target-projectile systems, the calculated loci of pairs of values a, $b(0)$ for which satisfactory fits to the data can be achieved. The widths of the shaded zones give the uncertainty associated with the experimental errors. The loci intersect at $a = 10.6$ MeV^{-1} and $b(0) = 7.5 \times 10^{-5}$ and nowhere else (excluding consideration of experimental error). In assigning experimental uncertainties to the values of a and $b(0)$ at the intersection, we used the rule-of-thumb that the standard error is roughly 0.71 of the extreme range of the region of overlap of the shaded zones, since the experimental errors for the two target-projectile systems are independent of each other. This gives $a = 10.6_{-2.0}^{+2.6}$ MeV^{-1} and $\log_{10} b(0) = -4.12_{-0.47}^{+0.28}$.

Effects of Varying Input Data

It is important to see how the position of the intersection is affected by reasonable changes in the input data. It is well known, for instance, that the Bjorklund-Fernbach set of optical-model parameters that we have used, which are for a surface-absorption model, is not a unique best set, that other sets, and even other forms of the optical model can do about as well in fitting the same scattering data.[33] We therefore recalculated the intersection values for a and $b(0)$ using the "volume absorption" optical model neutron transmission coefficients of Campbell et al.,[34] obtaining the result $a = 12.9$ MeV^{-1}, $b(0) = 3.7 \times 10^{-5}$. In another recalculation we used the probably unreasonably small moment of inertia of $\mathscr{I} = 0.3 \mathscr{I}_r$ in the level density expression, Eq. (8), and obtained the result $a = 11.3$ MeV^{-1}, $b(0) = 2.0 \times 10^{-4}$. We did not perform a careful recalculation with inclusion of a condensation energy[35]; however, rough calculations show that a condensation energy of[36,37] 0.8 MeV would reduce our value of a by

[30] J. R. Huizenga and G. Igo, Argonne National Laboratory, Argonne, Illinois, privately circulated report, 1961 (unpublished); see also J. R. Huizenga and G. Igo, Nucl. Phys. 29, 462 (1962).

[31] Nuclear Data Sheets, compiled by K. Way et al. (Printing and Publishing Office, National Academy of Sciences—National Research Council, Washington, D. C.); K. Way, N. B. Gove, C. L. McGinnis, and R. Nakasima, in Landolt-Börnstein, Energy Levels of Nuclei: A=5 to A=257, edited by A. M. Hellwege and K. H. Hellwege (Springer-Verlag, Berlin, 1961), Vol. I.

[32] This correction is discussed, and calculated values for some special cases are given, in the following papers: A. M. Lane and J. E. Lynn, Proc. Phys. Soc. (London) A70, 557 (1957); L. Dresner, Proceedings of the International Conference on the Neutron Interactions with the Nucleus, September, 1957 [Atomic Energy Commission Report TID-7547 (unpublished)], p. 71; P. A. Moldauer, Phys. Rev. 123, 968 (1961).

[33] See, for example, remarks by A. E. Glassgold, Progr. Nucl. Phys. 7, 123 (1959). It is instructive to compare the various sets of transmission coefficients with one another, all of which give fits to scattering data: e.g., Ref. 34; W. S. Emmerich, Fast Neutron Physics Part II, edited by J. B. Marion and J. L. Fowler (Interscience Publishers, Inc., New York, 1963), p. 1057; E. H. Auerbach and F. G. J. Perey, Brookhaven National Laboratory Report BNL-765, July 1962 (unpublished); J. R. Beyster, R. G. Schrandt, M. Walt, and E. W. Salmi, Los Alamos Scientific Laboratory Report LA-2099, April, 1957 (unpublished).

[34] E. J. Campbell, H. Feshbach, C. E. Porter, and V. F. Weiss-kopf, Massachusetts Institute of Technology Laboratory for Nuclear Science Technical Report No. 73, February 8, 1960 (unpublished). The transmission coefficients based on the above have been tabulated by P. A. Moldauer, Argonne National Laboratory Report ANL-6323, March 1961 (unpublished).

[35] H. Hurwitz, Jr. and H. A. Bethe, Phys. Rev. 81, 898 (1951).

[36] A. Stolovy and J. A. Harvey, Phys. Rev. 108, 353 (1957).

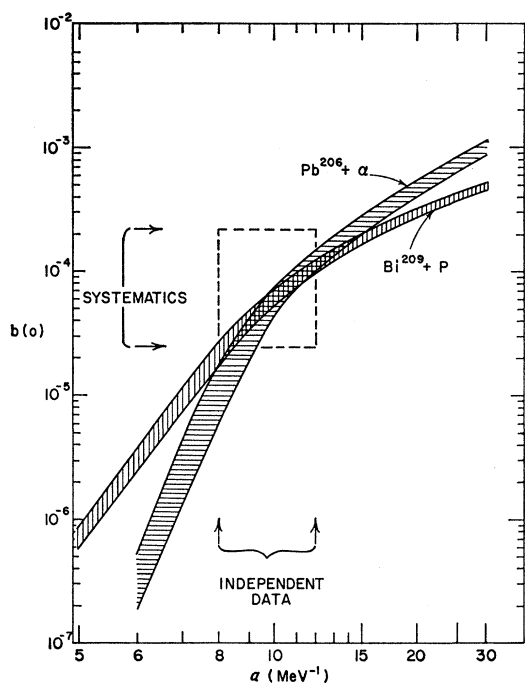[37] A. G. W. Cameron, Can. J. Phys. 36, 1040 (1958).

FIG. 4. Loci of pairs of values a and $b(0)$ for which calculated excitation functions fit the experimental data (see text).

only about 10% and cause a much smaller change in $b(0)$ than is caused when $\mathcal{I}_r$ is replaced by 0.3 $\mathcal{I}_r$.

One notices at once the insensitivity of a to these changes, compared to the great sensitivity of $b(0)$. This can be understood in the following way, using Eq. (18) of Ref. 1, and taking the following point of view of what this equation means. If the transmission coefficients are changed, or if $b(J)$ is changed (e.g., through a change in the value of $\mathcal{I}$), we can bring a given channel fraction k back to its original value by a suitable adjustment of $b(0)$. Now we can see from Fig. 3 that only the angular momentum $(\frac{5}{2})\hbar$, and to a lesser extent $(\frac{3}{2})\hbar$ and $(\frac{7}{2})\hbar$, in Po^{209}, are really sensitive to the input data, the values of k for the other angular momenta being either so near 1 or so near 0, that even fairly large changes in the input data do not vary them enough to matter. Thus, in effect, we need only return k for one angular momentum of Po^{209}, namely, for $J=\frac{5}{2}$, back to its original value by a suitable adjustment of $b(0)$, and the excitation function itself is returned to approximately its original position before the change in input data was made. Moreover, this is true for both excitation functions simultaneously, since identically the same channel fractions k apply to both (excluding the considerations expressed in footnote 12). The population distribution function S in Eq. (4) of Ref. 1 is scarcely changed at all by reasonable changes in the optical model transmission coefficients or in $\mathcal{I}$. This is because (1) the neutrons emitted from Po^{210} cause relatively little change in the distribution of the excited nuclei with respect to angular momentum, and changes in the

T_i's or in $\mathcal{I}$ cause only a small change in this already small change, (2) the distribution of the excited Po^{209} nuclei with respect to excitation energy depends mainly on a and on $\sum_{l=0}^{\infty} (2l+1)T_l$ and only weakly on $\mathcal{I}$ or on the exact values of the T_i's for individual partial waves.

Thus, we arrive at the important conclusion that a is determined by our experiment with reasonably good certainty, even if it turns out that we did not use exactly the correct optical-model parameters, or value of $\mathcal{I}$.

Comparison with Other Work

Also shown in Fig. 4 are the ranges of values of $b(0)$ and a which we believe reasonable, and which we use to construct a rectangle within which we would expect the intersection to occur. The range of acceptable values of $b(0)$ comes from the values of the mean gamma-ray emission width $\bar{\Gamma}_\gamma$ and of the mean level spacing, estimated using the systematics of Stolovy and Harvey,[36] and the calculational prescription of Cameron,[37] respectively (the value $b(0)=7.3\times10^{-5}$ corresponds roughly to $\bar{\Gamma}_\gamma=0.21$ eV). The range of acceptable values of a comes from seven values for the mass range $A=204$ to 210 calculated by D. W. Lang[38] for data he selected from the literature; four of these are calculated from direct counts of levels seen in slow-neutron work,[39] and the other three are derived from the results of inelastic neutron scattering experiments.[40] That our value of a is in agreement with other values obtained in this mass range from inelastic neutron scattering is especially interesting because our experiment effectively looks at the low-energy part of the neutron evaporation spectrum (from 0 to 0.6 MeV) which is not included in the usual measurements of neutron spectra, and hence is complementary to them.

We stress here that a, as determined in our experiment, applies to Po^{209} for excitation energies less than about 7.6 MeV.

The values of a predicted for our experiment by Newton's theory,[41] and by Lang's modification[38] of Newton's theory are 14.0 MeV^{-1} and 16.9 MeV^{-1}, respectively. Although these values seem a little high, their agreement with our experiment is as good as is the general agreement of this theory with much other experimental work over the entire spectrum of mass numbers (see Lang's Figs. 5 and 6 in Ref. 38).

Conclusions

The values of a and $b(0)$ that we obtain from our experiment seem quite reasonable, according to what

[38] D. W. Lang, Nucl. Phys. 26, 434 (1961).
[39] To compare with our work his values should be reduced by about 20%, because we neglect the condensation energy.
[40] The upward adjustment of these values for the neglect of condensation energy nearly cancels the downward adjustment, suggested by the work of T. D. Thomas, Nucl. Phys. (to be published), which results when angular momentum effects are more properly taken into account.
[41] T. D. Newton, Can. J. Phys. 34, 804 (1956).

the values obtained by other workers have led us to expect, so we have no evidence that we need a more complicated or sophisticated model than the compound nucleus model to explain our data. Since this conclusion is inextricably tied to our method of analyzing the experimental data, we also view the success of our analysis as evidence that (1) we have taken account of competitive gamma-ray emission reasonably correctly, and that (2) there remain no as-yet-overlooked effects of large importance for interpreting these data.

OTHER RESULTS AND COMMENTS

Error Analysis

In Table II are given, for $a = 10$ MeV^{-1}, the calculated values of $\log_{10} b(0)$ for one of the Pb$^{206}+\alpha$ runs and

TABLE II. Major sources of error in the determination of $b(0)$. Cited values are for $a = 10$ MeV^{-1}.

Target + projectile	$\log b(0)$	$W_{1/2}$	R_x First value above threshold	R_x higher value(s)	Ni Backing foil thickness	rms uncertainty
Pb$^{206}+\alpha$	−4.346	±0.050	±0.074	±0.048	±0.135	±0.170
Bi$^{209}+p$	−4.215	±0.009	±0.053	±0.044[a]	±0.018	±0.062

[a] Represents a typical value for an individual foil; the actual values for the three foils were ±0.054, ±0.033, and ±0.046.

for the lower-energy Bi$^{209}+p$ run. Columns three to six give a breakdown of the important sources of error[42] and the seventh column gives the resultant uncertainty in the knowledge of $\log b(0)$. For other values of a the sizes of the errors bear the same relative relationship to each other, but the over-all magnitude changes, as can be seen from Fig. 4 and Tables III and IV. The greatest single source of error in the α-particle irradiation of Pb^{206} is the uncertainty in the foil thickness seen by the beam, while the greatest error source for the proton irradiation of Bi^{209} is the counting statistics. We may partially check whether the results of our analysis of

TABLE III. Comparison of observed precision with error analysis for Pb$^{206}+\alpha$ system.

a (MeV^{-1})	$\log b(0)$ 1st bombardment	$\log b(0)$ 2nd bombardment	Uncertainty from precision	Uncertainty from error analysis
6	−6.68	−6.31	±0.19	±0.22
8	−5.18	−4.80	±0.19	±0.24
10	−4.35	−4.15	±0.10	±0.12
15	−3.68	−3.56	±0.06	±0.07
30	−3.05	−2.96	±0.05	±0.06

errors are reasonable by looking at the precision of replicate determinations. Since we did two Pb$^{206}+\alpha$ bombardments, we can compare the results, and this is done in Table III. Columns two and three give the values of $\log_{10} b(0)$ corresponding to values of a given in column one. Column four gives one-half the difference between columns two and three, which corresponds roughly to the standard error of the mean, and which is to be compared with the rms uncertainty derived from the direct-error analysis, in column five. We can check the Bi$^{209}+p$ data "internally," even though there was only one run, because we have four points at energies between threshold and $\mathscr{E} = 0.72$ MeV, and we only need two points to do a fitting. We calculated $b(0)$ separately at each a for the point nearest threshold plus each of the three higher points (we do not believe the second point above threshold plus a still higher point would make a good check, since the effects of the experimental errors are magnified in that case owing to the comparatively great distance of the lower point of the chosen pair from threshold) and the results are shown in Table IV, together with, in column six the resulting estimate of the standard error of the mean from the precision, and in column seven the corresponding estimate from the error analysis. We see that in both target-projectile systems, the uncertainties suggested by the estimates of precision are consistent with the results of the error analyses, so we believe that the latter are

TABLE IV. Comparison of observed precision with error analysis for Bi$^{209}+p$ system.

a (MeV^{-1})	Log $b(0)$ obtained from the 1st point above threshold and the 2nd point above threshold	3rd point above threshold	4th point above threshold	average $\log b(0)$	Uncertainty from precision	Uncertainty from error analysis
5	−6.27	−6.15	−6.05	−6.16	±0.08	±0.09
8	−4.56	−4.61	−4.84	−4.67	±0.10	±0.09
10	−4.21	−4.16	−4.28	−4.22	±0.04	±0.06
15	−3.79	−3.70	−3.72	−3.74	±0.03	±0.04
30	−3.36	−3.29	−3.30	−3.31	±0.02	±0.03

[42] We describe our error analysis in some detail because our early relatively intuitive error estimates proved quite untrustworthy; we have tried to give here, and in the Technical Details section, enough information to provide a reliable basis for designing future experiments.

essentially correct, and that no important source of error has been overlooked.

Extrapolation to Threshold

For the analysis reported here, it is important to find the threshold energy internally consistent with the experimental data, in order to apply the correction for the energy profile of the incident beam. If it were not for this correction, the threshold-energy determinations would be only incidental to the extraction of the parameters a and $b(0)$. We found that no simple extrapolation procedure was sufficiently accurate for our purpose, that the threshold energies have to be extracted using the full calculation, and that in fact the extrapolated threshold energies are functions of a and $b(0)$. Table V demonstrates this behavior of the ex-

TABLE V. Threshold energies (in MeV) determined by extrapolation of the data.[a]

a (MeV^{-1})	$Pb^{206}+\alpha$ 1st bombardment	$Pb^{206}+\alpha$ 2nd bombardment	$Bi^{209}+p$
5			9.695
6	20.125±0.016	20.092±0.016	
8	20.116±0.021	20.082±0.021	9.669
10	20.105±0.018	20.072±0.018	9.660±0.007
15	20.116±0.015	20.082±0.015	9.660
30	20.150±0.015	20.117±0.015	9.682

[a] Values listed are those corresponding to values of a in column one and the corresponding values of $b(0)$ as given in Tables III and IV.

trapolated thresholds. We include the estimated error arising only from those experimental uncertainties listed in Table II; i.e., the cited uncertainties are relevant only with respect to the energy differences within the pertinent foil stacks.

It is intriguing that the extrapolated threshold energy for each target-projectile system should go through a minimum near $a=10$ MeV^{-1}, which is just where we find the intersection of the loci in Fig. 4. We see no obvious reason for this behavior.

Comparison with the Data of Andre et al.

We analyzed the data of Andre et al.,[16] assuming $a=10$ MeV^{-1}, obtaining $E_{th}=9.46$ MeV, and $b(0)=7.2\times10^{-5}$ (We adjusted their energy scale to be consistent with the range-energy tables of Williams and Boujot[21].) The value of $b(0)$ that we obtained from their data is in quite good agreement with the value $b(0)=6.1\times10^{-5}$ that we obtained from our data for $a=10$ MeV^{-1}. Their data are plotted together with ours as a function of $(E_b+\Delta E)-E_{th}$, in Fig. 5; the agreement between the two experiments is entirely satisfactory.[43]

[43] The small disagreement between the shapes of the calculated excitation functions in Fig. 1 of Ref. 1 and Andre et al.'s data is removed when the new extrapolation method is used to find the threshold energy.
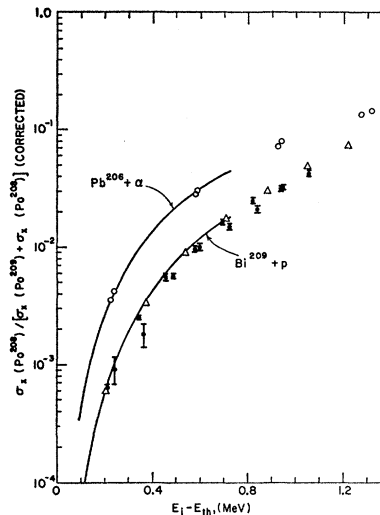

FIG. 5. Plot of $R_x=\sigma_x(Po^{208})/[\sigma_x(Po^{208})+\sigma_x(Po^{209})]$ versus E_i-E_{th} for the part of the excitation functions nearest threshold. The experimental data for the $Pb^{206}+\alpha$ system are given by circles and for the $Bi^{209}+p$ system by triangles; these data have been corrected for the energy-profile of the incident beam, i.e., $E_i=E_b+\Delta E$, assuming $a=10$ MeV^{-1}. The solid lines are calculated excitation functions for $a=10$ MeV^{-1}, $b(0)=5.7\times10^{-5}$, $s=s_r$ (i.e., inside the overlap zone of Fig. 4). The dots with error flags are the data of Andre et al. (Ref. 16) (see text).

Fig. 5 also serves to demonstrate the dramatic difference between the $Pb^{206}+\alpha$ and $Bi^{209}+p$ data near threshold.

Comment on a Puzzling Result in the Analysis of Some Nuclear Reaction Data

We here point out an unusual instance of difficulty arising in the analysis of some data on the reaction $Pb^{207}(\alpha,n)Po^{210}$ just above the threshold for the $Pb^{207}(\alpha,2n)Po^{209}$ reaction, which difficulty can almost surely be removed if competitive gamma-ray emission is taken into account. Morton and Harvey[44] measured the angular distributions of Po^{210} nuclei recoiling from very thin Pb^{207} targets under helium-ion bombardment at incident energies of 20 to 24 MeV, and then compared their data with theoretical angular distributions calculated assuming that the reaction proceeds by a compound nucleus mechanism in which neutrons are invariably emitted if the excited nucleus has sufficient excitation energy to emit them. They demonstrate that their calculation does not agree with the experimental data; several of their calculated angular distributions display a conspicuous maximum at angles of roughly 7 to 11 degrees (lab) in disagreement with their experimental curves, each of which shows instead a wider and much less prominent maximum at around 4 to 6°, with the experimental values then decreasing apparently monotonically toward larger angles. They

[44] J. R. Morton, III and B. G. Harvey, Phys. Rev. 126, 1798 (1962).

suggest that this disagreement between the experiments and calculations is probably evidence that the $Pb^{207}(\alpha,n)Po^{210}$ reaction occurs to a large extent by some direct interaction mechanism. However, from the results of our experiment involving the similar $Pb^{206}+\alpha$ system and the same energies it would seem unlikely that direct interaction mechanisms contribute very importantly. We offer the following alternative explanation of the disagreement between Morton and Harvey's experiments and calculations, an explanation which is entirely within the framework of the compound nucleus model.

The ground-state spin-parity of Po^{209} is $\frac{1}{2}-$, and the first excited state is thought to be at 0.78 MeV with a spin-parity of $\frac{3}{2}-$,[31] while the distribution of angular momenta in the Po^{211} compound nucleus should be quite similar to the curve shown in Fig. 2 for $Pb^{206}+\alpha$ since the spin of the Pb^{207} target is only $\frac{1}{2}$ and the incident energies are of similar magnitude to that assumed in preparing Fig. 2. Thus we expect, from the close similarity in these features to the $Pb^{206}(\alpha,2n)Po^{208}$ reaction with which we are already familiar, that above the $Pb^{207}(\alpha,2n)Po^{209}$ threshold there will be an appreciable contribution of Po^{210} nuclei to the reaction which had been sufficiently excited to emit a neutron, but which de-excited instead by gamma-ray emission. These particular excited Po^{210} nuclei are just the ones which are the result of the lowest energy neutron emissions from the Po^{211} compound nuclei, and hence contribute Po^{210} nuclei going only into the smallest angles. Viewed in this way, it is evident that the neglect of competitive gamma-ray emission would cause the calculated curves to disagree with the data because the loss of Po^{210} resulting from the formation of Po^{209} is overestimated, and consequently the relative height of the angular distribution near $0°$ is underestimated. As is expected with the above considerations, the spurious maxima appear only for incident energies above the threshold for the $Pb^{207}(\alpha,2n)Po^{209}$ reaction (19.83 MeV, c.m.), but not below this threshold, where the calculation predicts instead a wider, much less prominent maximum at smaller angles.

Remarks About the Formation of Po^{210}

For the $Bi^{209}+p$ bombardments, the observed Po^{210} comes from the $Bi^{209}(p,\gamma)$ reaction (as already mentioned, we were not troubled by deuteron contamination of the incident beam). We show, in Fig. 6 a plot of our measured values of $\mathfrak{R}_\gamma$ compared with the previously measured values of Kelly,[45] and of Andre et al.[16] Our data are in reasonable agreement with Kelly's, and in excellent agreement with those of Andre et al. The order of magnitude of the $Bi^{209}(p,\gamma)Po^{210}$ cross section at these energies has already been shown[46] to be in

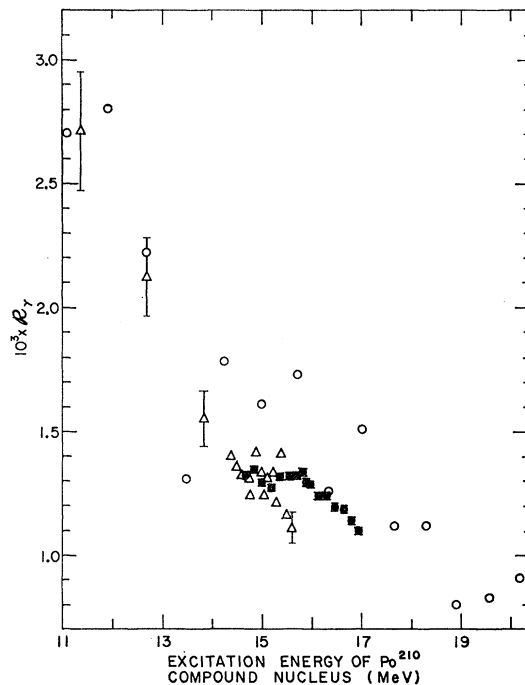[45] E. L. Kelly, University of California Radiation Laboratory Report UCRL-1044, 1950 (unpublished).
[46] A. M. Lane and J. E. Lynn, Nucl. Phys. 11, 646 (1959).

FIG. 6. Experimental values of $\mathfrak{R}_\gamma = \sigma_p(Po^{210})/[\sigma_p(Po^{210}) + \sigma_p(Po^{209}) + \sigma_p(Po^{208})]$ for the system $Bi^{209}+p$, versus the excitation energy of the Po^{210} compound nucleus. The large open circles are the data of Kelly (Ref. 45), the open triangles are the data of Andre et al. (Ref. 16), and the small closed circles with error flags are our data.

agreement with the compound nucleus model, with the direct-capture contribution becoming important at somewhat higher energies than our measurements reached. The flat shoulder appearing at excitation energies in the Po^{210} compound nucleus of 14.5 to 16 MeV, hints that there is interesting structure in this excitation function which would be revealed if work of precision comparable to ours were to be done extending the excitation function to lower and higher energies. Structures similar to this might possibly be explainable within the compound nucleus model, and could be associated with the second (and subsequent) steps in the gamma-ray cascade de-exciting the Po^{210} compound nucleus. Those Po^{210} compound nuclei which first gamma de-excite in competition with neutron emission will form excited residual Po^{210} nuclei in a rather sharply peaked spectrum of energies having a maximum a few MeV lower than the energy of the compound nucleus. If the energy of the compound nucleus is such that this maximum occurs near the energy at which neutron emission begins to compete effectively with gamma-ray emission, $\mathfrak{R}_\gamma$ will display a rather precipitous drop, compared with its behavior at energies only a few MeV away on either side. However, with such a qualitative argument we cannot tell whether one could predict the values of $\mathfrak{R}_\gamma$ to be as nearly constant over a zone at least 1.5 MeV wide, as we observed in this experiment.

For the $Pb^{206}+\alpha$ bombardments, the observed Po^{210} comes not only from the $Pb^{206}(\alpha,\gamma)Po^{210}$ reaction but also from the $Pb^{207}(\alpha,n)Po^{210}$ and $Pb^{208}(\alpha,2n)Po^{210}$ reactions induced in the Pb^{207} and Pb^{208} impurities in our targets. We inadvertently exposed several foils of the first bombardment to contamination with natural lead, and a comparison of $\mathfrak{R}_\gamma$ values in Table I indicates that slight contamination of some of the foils in the first bombardment occurred. In addition, there were also other risks of contamination of our targets with natural lead, especially in the chemical manipulations of the separated Pb^{206} associated with the electroplating procedure, even through great care was taken, so we should not be too surprised to discover that the nominal 0.15% content of Pb^{207} reported by Oak Ridge is too low. If we assume that $\mathfrak{R}_\gamma(Bi^{209}+p)=\mathfrak{R}_\gamma(Pb^{206}+\alpha)$, where $\mathfrak{R}_\gamma(Pb^{206}+\alpha)$ refers only to Po^{210} produced in the α,γ reaction, and ascribe the difference entirely to Pb^{207} impurity, we obtain about 0.4 atom percent of "Pb^{207}" for the first bombardment and about 0.26% for the second.

ACKNOWLEDGMENT

APPENDIX

The Beam Energy-Profile Correction

For two experimental values of R_x and an assumed value of a, we can find those values of $b(0)$ and of the threshold energy E_{th} for which our calculated excitation function reproduces the values of R_x. However, this technique of analysis is complicated by the necessity to correct the experimental data for the effect of the energy inhomogeneity of the incident beam as seen by each foil.

Since practically all of the beam-profile correction applies to the steeply rising and sharply curved excitation function for the production of Po^{208}, and much less to the more leisurely rising and more gently curved excitation function for the production of Po^{209}, we calculated the correction only for the Po^{208} excitation function. We estimated the excitation function for the formation of Po^{208} through the relation

$$\sigma_x(Po^{208})=R_x\pi\lambda_x^2\sum_{l=0}^{\infty}(2l+1)T_l,$$

where λ_x is the de Broglie wavelength of the incident projectile divided by 2π, and the T_l's are the appropriate optical-model transmission coefficients already mentioned. We found that the energy dependence of $\sigma_x(Po^{208})$ in the threshold region of concern to us could be given to a good approximation by the empirical relation

$$\sigma_x(Po^{208})\propto(E_i-E_{th})^m,$$

where $E_i\geqslant E_{th}$ is the c.m. incident energy, and m is energy-independent but otherwise is a function of a, $b(0)$, and of the target-projectile system. We assumed a Gaussian shape for the beam profile

$$S_x(E_b,E_i)\propto\exp-(E_i-E_b)^2/2w^2,$$

where $w=W_{1/2}/(8\ ln\ 2)^{1/2}=W_{1/2}/2.354$ and E_b is the nominal bombarding energy as listed in column two of Table I. When $W_{1/2}>0$ and $m>1$ the observed cross section is apparently too large, if one sets $E_i=E_b$, and must be corrected downward, or, conversely, the energy associated with the observed cross section is apparently too small, and one could add a corrective term ΔE to E_b to find an effective value of E_i corresponding to the

TABLE VI. Table for calculating values of ΔE.

m \ $[E_b-E_{th}]/W_{1/2}$	0.05	0.15	0.25	0.50	0.75	1.00	1.50	2.00	2.50
1.75	0.2511	0.2131	0.1810	0.1230	0.0881	0.0670	0.0449	0.0337	0.0270
2.00	0.2792	0.2415	0.2093	0.1490	0.1107	0.0863	0.0590	0.0446	0.0358
2.25	0.3052	0.2677	0.2352	0.1731	0.1319	0.1046	0.0726	0.0553	0.0445
2.50	0.3294	0.2919	0.2593	0.1956	0.1519	0.1221	0.0860	0.0658	0.0532
2.75	0.3521	0.3147	0.2818	0.2167	0.1710	0.1389	0.0990	0.0762	0.0617
3.00	0.3735	0.3362	0.3031	0.2368	0.1892	0.1551	0.1117	0.0864	0.0701
3.25	0.3939	0.3566	0.3233	0.2559	0.2067	0.1708	0.1242	0.0965	0.0785

observed cross section; i.e., $E_i = E_b + \Delta E$. We find the latter view the more useful and opted to calculate amounts of energy ΔE which should be added to E_b at each point to correct for the spread of the beam. For use in making this correction we calculated a fine-meshed table of ΔE, part of which is reproduced as Table VI. The entries therein are given as values of $\Delta E / W_{1/2}$. For energies higher than the range of the table, a reasonably accurate approximation to use is

$$\frac{\Delta E}{W_{1/2}} \propto \left(\frac{E_b - E_{th}}{W_{1/2}} \right)^{-1} .$$

Our specific calculational procedure was as follows: (1) From the raw data (or, better, using reasonable guesses for values of ΔE) obtain preliminary values of $b(0)$ and E_{th} for a given value of a; (2) using the two data points and this first approximation to E_{th} calculate m; (3) using m and the known values of $W_{1/2}$ for each data point obtain the corresponding values of ΔE from the table; (4) using these values of ΔE to correct the energies E_b associated with the data points, go back and calculate improved values of $b(0)$ and E_{th}, and so on. We showed that our procedure converges rapidly to the same point from both directions.

Differential Range Study of Products Formed by 2.9-GeV Proton Irradiation of Silver*

J. B. CUMMING, S. KATCOFF, N. T. PORILE, S. TANAKA,† AND A. WYTTENBACH‡

Chemistry Department, Brookhaven National Laboratory, Upton, New York

(Received 31 January 1964)

Thin silver targets (≈ 0.1 mg/cm²) were irradiated with 2.9-GeV protons. The recoiling products were collected in a stack of thin plastic films at 90° to the beam, at a geometry of 2%. By radiochemical separation Sr^{83}, $Cu^{61,64}$, $Sc^{43,44}$, $K^{42,43}$, and Na^{24} were removed from the films. Range distributions were obtained for each, and from these the corresponding energy spectra and velocity spectra were deduced. The mean energies are: Sr^{83}—3.2 MeV, $Cu^{61,64}$—5.9 MeV, $Sc^{43,44}$—9.4 MeV, Na^{24}—18.1 MeV. Comparison of the observed spectra with the results of Monte Carlo cascade-evaporation calculations showed excellent agreement for all of the products except Na^{24}. It is concluded that the former are mainly spallation residues while Na^{24} is formed by the splitting of a parent nucleus into two fragments. All of the energy spectra are very broad and there is no sharp difference between "spallation-type" spectra and "two-body breakup" type spectra.

INTRODUCTION

THERE has been extensive discussion in the literature[1-4] about the mechanisms involved in high-energy nuclear reactions. For the production of species not too far removed from medium weight targets it is generally agreed that a two-step, cascade-evaporation, process predominates. Monte Carlo calculations based on this model[5,6] give mass-yield curves which are in fair agreement with experiment down to products whose mass is about half that of the target nuclei. Species substantially lighter than half the target mass are most

probably produced by some other mechanisms, those involving break up into two bodies. This has often been called[2-4,7,8] "fragmentation." It is thought to occur at a time very close to that of the fast nucleon cascade. The term "fission" used for heavy elements has also been applied[8-12] to a two body breakup of medium weight elements, but then one usually thinks of a longer time scale, comparable with evaporation times. Numerous experiments[2-4,7] have been interpreted by means of the fragmentation mechanism. In a recent nuclear emulsion investigation[12] evidence was presented for a mechanism more properly called "fission."

In the present work, recoil range distributions were obtained for a series of products of widely differing

* Research performed under the auspices of the U. S. Atomic Energy Commission.

† Present address: Institute for Nuclear Study, Tokyo University, Tokyo, Japan.

‡ Present address: Eidg. Institut für Reactorforschung, Würenlingen AG, Switzerland.

[1] J. M. Miller and J. Hudis, Ann. Rev. Nucl. Sci. 9, 159 (1959).

[2] R. Wolfgang, E. W. Baker, A. A. Caretto, Jr., J. B. Cumming, G. Friedlander, and J. Hudis, Phys. Rev. 103, 394 (1956).

[3] V. P. Crespo, J. M. Alexander, and E. K. Hyde, Phys. Rev. 131, 1765 (1963).

[4] J. B. Cumming, R. J. Cross, Jr., J. Hudis, and A. M. Poskanzer, Phys. Rev. 134, B167 (1964).

[5] N. Metropolis, R. Bivins, M. Storm, J. M. Miller, G. Friedlander, and A. Turkevich, Phys. Rev. 110, 204 (1958).

[6] N. T. Porile (unpublished evaporation calculation for spallation of Ag by 1.8-GeV protons).

[7] A. A. Caretto, Jr., J. Hudis, and G. Friedlander, Phys. Rev. 110, 1130 (1958).

[8] N. A. Perfilov, O. V. Lozhkin, and V. P. Shamov, Usp. Fiz. Nauk. 70, 3 (1960) [English transl.: Soviet Phys.—Usp. 3, 1 (1960)].

[9] G. F. Denisenko, N. S. Ivanova, N. R. Novikova, N. A. Perfilov, E. I. Prokoffieva, and V. P. Shamov, Phys. Rev. 109, 1779 (1958).

[10] K. W. Rind, thesis, Columbia University, New York, July 1961 (unpublished).

[11] E. W. Baker and S. Katcoff, Phys. Rev. 123, 641 (1961).

[12] E. W. Baker and S. Katcoff, Phys. Rev. 126, 729 (1962).